INTERNATIONAL JOURNAL FOR NUMERICAL METHODS IN FLUIDS
Int. J. Numer. Meth. Fluids 2008; **56**:1047–1059
Published online 8 December 2007 in Wiley InterScience (www.interscience.wiley.com). DOI: 10.1002/fld.1697

A fully implicit, mass-conserving, semi-Lagrangian scheme for the f-plane shallow-water equations

J. Thuburn*, †

Mathematics Research Institute, School of Engineering, Computer Science and Mathematics, University of Exeter, EX4 4QF, U.K.

SUMMARY

A fully implicit, mass-conserving, semi-Lagrangian discretization of the shallow-water equations on a doubly periodic f-plane is proposed. The scheme requires the solution of a nonlinear and nonlocal system of equations at each time step. When a Newton method is used to solve this system of equations, a partial elimination of the unknowns can be carried out to leave a near standard elliptic problem at each Newton iteration, for which efficient solution methods are well known. Moreover, the nonlinearity is, in fact, rather weak so that a small number of Newton iterations (1–3) should be sufficient for practical application.

Setting up the Newton method and solving the resulting elliptic problem can be made cheaper by making certain approximations to the terms in the Jacobian matrix; the price to pay is a slowing of the Newton convergence rate. Numerical experiments are carried out to quantify the effects on convergence rate of such approximations to help decide the optimum trade-off between cost per Newton iteration and iteration count. Copyright © 2007 John Wiley & Sons, Ltd.

Received 27 April 2007; Revised 26 October 2007; Accepted 26 October 2007

KEY WORDS: Newton method; approximate Jacobian; Helmholtz problem; SLICE; implicit; nonlinear solver

1. INTRODUCTION

This paper considers how to combine several numerical techniques with the aim of developing a more accurate and efficient dynamical core for weather and climate prediction models. The techniques in question are (i) the use of a staggered grid, (ii) the use of implicit time stepping, and (iii) the use of a mass-conserving semi-Lagrangian advection scheme. Each of these techniques is considered advantageous. However, combining the three of them poses considerable technical

*Correspondence to: J. Thuburn, Mathematics Research Institute, School of Engineering, Computer Science and Mathematics, University of Exeter, EX4 4QF, U.K.
†E-mail: j.thuburn@exeter.ac.uk

Contract/grant sponsor: Met Office

challenges, and to date there have been few attempts to do so; one such attempt for the shallow-water equations is described by Lauritzen *et al.* [1]. Particular features of the scheme proposed here are that it avoids the introduction of a reference geopotential in the mass equation and that it avoids the use of any time-extrapolated terms, instead treating all terms in a Crank–Nicolson manner; in this sense it is *fully* implicit.

An implicit time stepping treatment of fast waves requires that, among others, the term involving the flow divergence in the mass equation must be handled implicitly, i.e. as a time average involving the unknown velocities at the new time level. When the mass equation is discretized using a conservative semi-Lagrangian scheme, however, the flow divergence appears only in the way the trajectories determine Lagrangian departure control volumes; therefore, the trajectories must be computed implicitly. This then leads to a coupled, nonlinear and nonlocal system of equations for the mass and velocity fields at the new time level. A Newton method may be used to solve this system of equations. Moreover, a partial elimination may be performed on the Newton iteration formulas to leave a near standard Helmholtz equation for the mass increment. A complete elimination of the velocity increments is not possible without approximation because of the use of the staggered grid. These issues are discussed in more detail below.

The Newton method requires the elements of a Jacobian matrix to be computed at each iteration, which is relatively expensive. It might be cost effective to approximate the Jacobian matrix, even if this leads to more Newton iterations being required. Three groups of approximations are discussed below, along with the parameter regimes in which they are expected to be valid. The effect on the Newton convergence rate of each group of approximations is investigated empirically for different flow regimes.

2. KEY ASPECTS OF THE PROPOSED SCHEME

2.1. The rotating shallow-water equations

The rotating shallow-water equations have many features in common with the full three-dimensional rotating compressible Euler equations, including fast divergent waves, slow, balanced vortical motions, and analogous conservation properties. For this reason, they are often used as a testbed for numerical methods before extending those methods to more complete equation sets (e.g. [2]). Here, we consider the solution of the f-plane shallow-water equations in doubly periodic Cartesian geometry, neglecting orography:

$$\frac{\mathrm{D}\Phi}{\mathrm{D}t}+\Phi\nabla\cdot\mathbf{v}=0 \tag{1}$$

$$\frac{\mathrm{D}u}{\mathrm{D}t}-fv+\Phi_x=0 \tag{2}$$

$$\frac{\mathrm{D}v}{\mathrm{D}t}+fu+\Phi_y=0 \tag{3}$$

Here, $\mathbf{v}=(u,v)$ is the velocity vector, Φ is the geopotential (proportional to fluid depth), f is the constant Coriolis parameter, $\mathrm{D}/\mathrm{D}t$ is the material derivative, and subscripts x and y indicate spatial partial derivatives.

DOI: 10.1002/fld

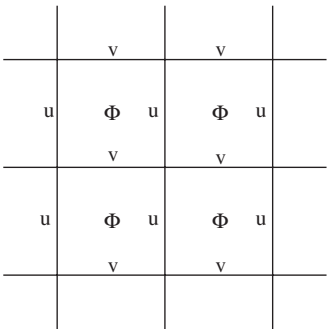

Figure 1. Schematic showing the distribution of variables on the staggered C-grid. Φ is located at cell centres, and normal velocity components are located at cell edges.

2.2. The C-grid

Although fast waves (acoustic and inertio-gravity waves) are observed to be energetically weak in the atmosphere on large scales, radiation of these waves is the mechanism through which the large-scale flow adjusts towards and remains close to hydrostatic and geostrophic balance. It is considered crucial that the fast waves, and hence the adjustment process, be captured sufficiently accurately. On smaller horizontal scales, inertio-gravity waves can be significant features of the flow; hence, it is important to capture them accurately in high-resolution models. For the horizontal discretization, the staggered C-grid (Figure 1) does significantly better than an unstaggered grid at capturing the fast waves, provided the grid spacing is smaller than the Rossby radius: $\Delta x < \Phi^{1/2}/f$ [3].

2.3. Implicit time stepping

The fast waves supported by the governing equations would require a very short time step for stability if an explicit time stepping scheme were used. Longer time steps are possible with an implicit time scheme. To avoid the need to solve a coupled nonlinear system of equations for the unknowns at each time step, it is common to use a *semi-implicit* time scheme [4], in which the terms responsible for the fast waves are split into a large part linearized about some reference state and a small remainder; only the linearized parts are then handled implicitly, leading to a linear system for the unknowns at each time step. A typical semi-implicit (nonconservative) semi-Lagrangian time scheme for the shallow-water equations is the following:

$$\frac{\Phi^{\mathrm{A}}-\Phi^{\mathrm{D}}}{\Delta t}+\frac{\Phi_0}{2}(\nabla\cdot\mathbf{v}^{\mathrm{A}}+\nabla\cdot\mathbf{v}^{\mathrm{D}})+\{(\Phi-\Phi_0)\nabla\cdot\mathbf{v}\}^*=0 \tag{4}$$

$$\frac{\mathbf{v}^{\mathrm{A}}-\mathbf{v}^{\mathrm{D}}}{\Delta t}+f\hat{\mathbf{k}}\times\mathbf{v}^*+\frac{1}{2}(\nabla\Phi^{\mathrm{A}}+\nabla\Phi^{\mathrm{D}})=0 \tag{5}$$

where the trajectory departure points are calculated using

$$\mathbf{x}^{\mathrm{D}}=\mathbf{x}^{\mathrm{A}}-\mathbf{v}^*\Delta t \tag{6}$$

Here, superscript A indicates a value at a trajectory arrival point (i.e. on the regular grid) at the new time level and superscript D indicates a value at a trajectory departure point at the old time level.

DOI: 10.1002/fld

Φ_0 is a constant reference geopotential, and $\hat{\mathbf{k}}$ is the unit vertical vector. Superscript $*$ indicates values to be estimated at the midpoint, in space and time, of the trajectory. These may, for example, be evaluated explicitly by a time extrapolation from earlier time levels. Because trajectory departure points and midpoints do not lie on the regular grid, values there must be evaluated by interpolation in space [5].

To step forward in time, $\mathbf{v}^{\mathrm{A}}$ is eliminated to leave a Helmholtz equation for Φ^{A}:

$$\nabla^2\Phi^{\mathrm{A}} - \nu^2\Phi^{\mathrm{A}} = \mathrm{RHS} \tag{7}$$

where ν^2 is a positive constant and RHS indicates terms that can be calculated straightforwardly from known quantities.

One drawback of the semi-implicit scheme is that the reference geopotential must be chosen carefully for stability and accuracy, e.g. [5]. Also, although the divergence term in the mass equation and the geopotential gradient term in the momentum equation are the most crucial for a stable treatment of the fast waves, there is some evidence that one could improve stability and robustness, better capture the balance among the dominant terms in the equations, and improve the coupling to other processes represented by sub-grid models, by using a more fully implicit time scheme (e.g. [6]).

2.4. Conservative semi-Lagrangian advection

A semi-Lagrangian treatment of advection (e.g. [5]) is widely used in atmospheric models, because the stability restriction on the permitted time step is much weaker than with explicit Eulerian advection schemes. However, the conventional formulation based on pointwise interpolation is not conservative. Local conservation of mass and of long-lived chemical species is considered important for climate simulation. This has stimulated the development of several semi-Lagrangian-like schemes that are conservative while retaining stability for large time steps [7–10].

In this paper we use the SLICE scheme [10, 11] for the advection of the mass field. At each step, the mass field must be conservatively remapped from the regularly arranged Eulerian control volumes to the Lagrangian departure control volumes. The two-dimensional remapping is carried out efficiently by decomposing it into two one-dimensional remappings using the 'cascade' method.

The conservative semi-Lagrangian discretization of the mass equation may then be expressed as

$$(\Phi\alpha)^{\mathrm{A}} - (\Phi\alpha)^{\mathrm{D}} = 0 \tag{8}$$

where α refers to the area of the arrival or departure control volume, depending on its superscript.

Note that a correct C-grid implementation of SLICE requires that the Lagrangian departure control volumes are constructed using cell-edge-centre trajectory departure points rather than cell corner trajectory departure points.

3. DISCRETIZATION

Motivated by the preceding discussion, the following fully implicit mass-conserving semi-Lagrangian time discretization is proposed. It is very similar to the shallow-water version of a scheme currently being developed at the Met Office, except that it avoids the introduction of a

DOI: 10.1002/fld

reference geopotential in the mass equation:

$$(\Phi\alpha)^{\mathrm{A}} - (\Phi\alpha)^{\mathrm{D}} = 0 \tag{9}$$

$$\frac{\mathbf{v}^{\mathrm{A}} - \mathbf{v}^{\mathrm{D}}}{\Delta t} + f\hat{\mathbf{k}} \times \frac{1}{2}(\mathbf{v}^{\mathrm{A}} + \mathbf{v}^{\mathrm{D}}) + \frac{1}{2}(\nabla\Phi^{\mathrm{A}} + \nabla\Phi^{\mathrm{D}}) = 0 \tag{10}$$

where

$$\mathbf{x}^{\mathrm{D}} = \mathbf{x}^{\mathrm{A}} - \frac{\Delta t}{2}(\mathbf{v}^{\mathrm{A}} + \mathbf{v}^{\mathrm{D}}) \tag{11}$$

The mass equation is to be solved using the conservative SLICE scheme, and all terms in the momentum and trajectory equations are to be handled fully implicitly. In particular, in contrast to semi-implicit schemes, no reference value Φ_0 is needed.

Discretizing in space, (9) and (10) may be expressed as

$$\mathbf{G} \equiv (G_\Phi, G_u, G_v) = 0 \tag{12}$$

where

$$G_\Phi = \frac{1}{\alpha^{\mathrm{A}}}\{(\Phi\alpha)^{\mathrm{A}} - (\Phi\alpha)^{\mathrm{D}}\} \tag{13}$$

$$G_u = \left\{u + \frac{\Delta t}{2}(-f\overline{v} + \delta_x\Phi)\right\}^{\mathrm{A}} - R_u^{\mathrm{D}} \quad \text{where } R_u = \left\{u - \frac{\Delta t}{2}(-f\overline{v} + \delta_x\Phi)\right\} \tag{14}$$

$$G_v = \left\{v + \frac{\Delta t}{2}\left(f\overline{u} + \delta_y\Phi\right)\right\}^{\mathrm{A}} - R_v^{\mathrm{D}} \quad \text{where } R_v = \left\{v - \frac{\Delta t}{2}\left(f\overline{u} + \delta_y\Phi\right)\right\} \tag{15}$$

An overline indicates a four-point spatial average to transfer fields between u and v points on the C-grid, while δ_x and δ_y indicate spatial finite difference approximations to $\partial/\partial x$ and $\partial/\partial y$.

The departure control volume terms in the mass equation (13) are evaluated using SLICE, as described above. The departure point terms in the momentum equation (14) and (15) are evaluated using cubic Lagrange interpolation. The departure point velocity in the trajectory equation (11) is evaluated using linear interpolation [5].

4. NEWTON METHOD-BASED SOLVER

The discretization presented above constitutes a nonlinear and nonlocal coupled system of equations for the unknowns $\mathbf{s} \equiv (\Phi^{\mathrm{A}}, u^{\mathrm{A}}, v^{\mathrm{A}})$. A standard iterative method of solving such systems of equations is Newton's method:

$$\mathbf{s}^{m+1} = \mathbf{s}^m + \mathbf{s}' \tag{16}$$

where the increment $\mathbf{s}' \equiv (\Phi', u', v')$ satisfies

$$(\nabla_{\mathbf{s}}\mathbf{G})\mathbf{s}' = -\mathbf{G}^m \tag{17}$$

$\nabla_{\mathbf{s}}\mathbf{G}$ is the Jacobian matrix and superscript m is the iteration count. However, the linear system (17) that must be solved at each Newton iteration is very large; hence, it must be solved very efficiently

DOI: 10.1002/fld

for this approach to be feasible. A key result here is that we can make a partial elimination of u' and v' in (17) to leave something resembling a standard Helmholtz problem for Φ', for which efficient solution methods are well known. Some details are described below.

The derivative of G_u (see (14)) with respect to Φ^{A} will clearly have contributions coming from the $\delta_x\Phi$ term at the arrival point. The derivative of G_u with respect to u^{A} will have a contribution coming directly from the arrival-point terms. However, the location of the departure point also depends on u^{A} through (11); hence, the derivative of G_u with respect to u^{A} will also have a contribution coming from $\partial\mathbf{x}^{\mathrm{D}}/\partial u^{\mathrm{A}}$ times the spatial gradient of R_u at the departure point. Similarly, the derivative of G_u with respect to v^{A} will include a contribution coming directly from the arrival-point Coriolis term and a contribution coming from the spatial gradient of R_u at the departure point. Hence, the components of (17) coming from the equations involving G_u are

$$\frac{\Delta t}{2\Delta x}\delta_x\Phi'+u'\left(1-\frac{\partial R_u^{\mathrm{D}}}{\partial x^{\mathrm{D}}}\frac{\partial x^{\mathrm{D}}}{\partial u^{\mathrm{A}}}-\frac{\partial R_u^{\mathrm{D}}}{\partial y^{\mathrm{D}}}\frac{\partial y^{\mathrm{D}}}{\partial u^{\mathrm{A}}}\right)$$
$$+\overline{v}'\left(-\frac{f\Delta t}{2}-\frac{\partial R_u^{\mathrm{D}}}{\partial x^{\mathrm{D}}}\frac{\partial x^{\mathrm{D}}}{\partial \overline{v}^{\mathrm{A}}}-\frac{\partial R_u^{\mathrm{D}}}{\partial y^{\mathrm{D}}}\frac{\partial y^{\mathrm{D}}}{\partial \overline{v}^{\mathrm{A}}}\right)=-G_u \tag{18}$$

A similar calculation gives the components of (17) coming from the equations involving G_v:

$$\frac{\Delta t}{2\Delta y}\delta_y\Phi'+v'\left(1-\frac{\partial R_v^{\mathrm{D}}}{\partial x^{\mathrm{D}}}\frac{\partial x^{\mathrm{D}}}{\partial v^{\mathrm{A}}}-\frac{\partial R_v^{\mathrm{D}}}{\partial y^{\mathrm{D}}}\frac{\partial y^{\mathrm{D}}}{\partial v^{\mathrm{A}}}\right)$$
$$+\overline{u}'\left(\frac{f\Delta t}{2}-\frac{\partial R_v^{\mathrm{D}}}{\partial x^{\mathrm{D}}}\frac{\partial x^{\mathrm{D}}}{\partial \overline{u}^{\mathrm{A}}}-\frac{\partial R_v^{\mathrm{D}}}{\partial y^{\mathrm{D}}}\frac{\partial y^{\mathrm{D}}}{\partial \overline{u}^{\mathrm{A}}}\right)=-G_v \tag{19}$$

The coefficients $\partial x^{\mathrm{D}}/\partial u^{\mathrm{A}}$, etc., are obtained by differentiating (11), recalling that $\mathbf{v}^{\mathrm{D}}$ is a function of $\mathbf{x}^{\mathrm{D}}$ given by the linear interpolation. The coefficients $\partial R_u^{\mathrm{D}}/\partial x^{\mathrm{D}}$, etc., are obtained by differentiating the cubic Lagrange interpolation formulas for R_u, etc.

We also require the components of (17) coming from equations involving G_Φ. Because SLICE involves a somewhat complicated geometrical construction of the departure and intermediate control volumes and because it involves a nonlocal parabolic spline remapping, an exact linearization would be complicated and nonlocal. However, to a very good approximation, the sensitivity of the mass in the departure cell to the location of one of the cell edges is given by the mean value of Φ on that edge times the length of that edge times a geometrical factor accounting for the direction of displacement. Thus, these components of (17) may be expressed as

$$\Phi'-\frac{1}{\alpha^{\mathrm{A}}}\left\{\delta_x\left[\left(\frac{\partial m}{\partial x}\frac{\partial x^{\mathrm{D}}}{\partial u^{\mathrm{A}}}+\frac{\partial m}{\partial y}\frac{\partial y^{\mathrm{D}}}{\partial u^{\mathrm{A}}}\right)u'+\left(\frac{\partial m}{\partial x}\frac{\partial x^{\mathrm{D}}}{\partial \overline{v}^{\mathrm{A}}}+\frac{\partial m}{\partial y}\frac{\partial y^{\mathrm{D}}}{\partial \overline{v}^{\mathrm{A}}}\right)\overline{v}'\right]\right.$$
$$\left.+\delta_y\left[\left(\frac{\partial m}{\partial x}\frac{\partial x^{\mathrm{D}}}{\partial \overline{u}^{\mathrm{A}}}+\frac{\partial m}{\partial y}\frac{\partial y^{\mathrm{D}}}{\partial \overline{u}^{\mathrm{A}}}\right)\overline{u}'+\left(\frac{\partial m}{\partial x}\frac{\partial x^{\mathrm{D}}}{\partial v^{\mathrm{A}}}+\frac{\partial m}{\partial y}\frac{\partial y^{\mathrm{D}}}{\partial v^{\mathrm{A}}}\right)v'\right]\right\}=-G_\Phi \tag{20}$$

The terms $\partial m/\partial x$ and $\partial m/\partial y$ are the rate of change of mass $(\Phi\alpha)^{\mathrm{D}}$ in the departure control volume when the cell edge in question is displaced in the x or y direction. They can be evaluated by an extension of the SLICE algorithm, using information that is a by-product of the parabolic spline remapping.

DOI: 10.1002/fld

Thus, Equations (18)–(20) constitute a linear system for Φ', u', and v' in which all the coefficients can be calculated. An efficient way to solve the linear system is to carry out analytically a partial elimination of the u' and v' terms. (Unfortunately, the $\overline{u}'$ and $\overline{v}'$ terms that arise because of the C-grid staggering cannot easily be eliminated without making some approximation.) This partial elimination leads to a Helmholtz problem:

$$\Phi' + \delta_x(A\delta_x\Phi') + \delta_y(D\delta_y\Phi') = -R - \delta_x(B\overline{v}') - \delta_y(C\overline{u}') \tag{21}$$

where

$$R = G_\Phi + \delta_x(A\tilde{G}_u) + \delta_y(D\tilde{G}_v) \tag{22}$$

coupled to update equations for u' and v'

$$u' = -E\tilde{G}_u - E\delta_x\Phi' - F\overline{v}' \tag{23}$$

$$v' = -H\tilde{G}_v - H\delta_y\Phi' - G\overline{u}' \tag{24}$$

Here, $\tilde{G}_u$ and $\tilde{G}_v$ are rescaled versions of G_u and G_v, and the coefficients $A, \ldots, G$ are easily determined from those in (18)–(20).

A number of efficient methods are available for the solution of equations like (21). Here, a full multigrid method is used [12]. At each smoothing iteration, u' and v' are updated using (23) and (24), allowing the right-hand side of (21) to be recomputed. The coefficients B, C, F, and G in the terms involving $\overline{u}'$ and $\overline{v}'$ in (21), (23), and (24) are small in practice; hence, this repeated updating of the right-hand sides does not adversely affect the multigrid convergence.

There is no guarantee of mass conservation under incomplete convergence of the Helmholtz problem (21)–(24), although in practice the errors have been found to be extremely small. If exact conservation to machine precision is required, then, after solving (21)–(24), the updated velocity field may be used in (9) to produce a final updated mass field.

5. SAMPLE RESULTS

The scheme described above has been implemented and tested on a number of test problems. It is found to have good stability properties, even for large wave and advective Courant numbers.

Figure 2 shows the results of one test case. The domain is $10^7\,\mathrm{m} \times 10^7\,\mathrm{m}$ with resolution 128×128 grid cells. The initial wind field consists of alternating jets in the positive and negative x direction, in geostrophic balance with the Φ field: $fu + \Phi_y = 0$. Such a flow field is a steady solution of the governing equations, and the numerical solution is also steady. To make the problem nontrivial, the initial Φ field is perturbed by adding a large spike at a single grid cell near the centre of the domain. The perturbation is advected by the jets and disperses by radiating inertio-gravity waves, which are clearly visible in the v field (Figure 2). Three Newton iterations are used at each step. The time step is 900 s making the wave Courant number about 4.0 and the maximum advective Courant number about 2.9.

Figure 3 shows another test case, this time with initially balanced jets that meander. These jets are fluid dynamically unstable and role up into two pairs of coherent vortices. There is strong straining between the vortices, which generates small-scale filamentary structure in the materially conserved potential vorticity field $q \equiv (f + v_x - u_y)/\Phi$. Again the resolution is 128×128 and three

DOI: 10.1002/fld

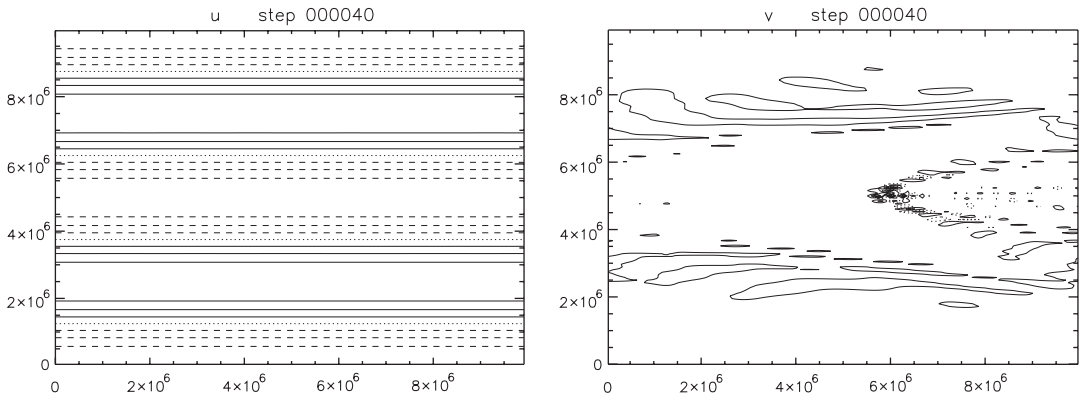

Figure 2. Test case in which initial balanced jets are perturbed by a spike in the Φ field. Left: u field after 40 steps; the maximum value is $251\,\mathrm{m\,s^{-1}}$; dashed contours indicate negative values; solid contours indicate positive values. Right: v field after 40 steps; peak values are of order $1\,\mathrm{m\,s^{-1}}$.

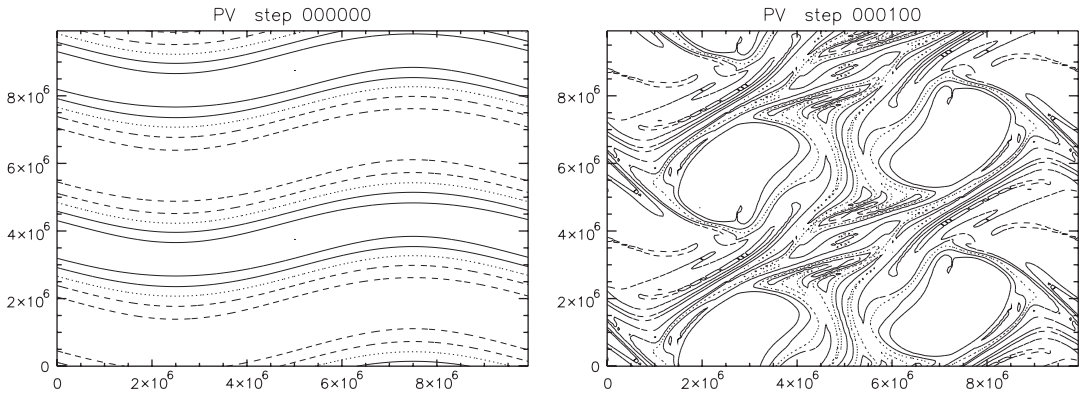

Figure 3. Test case with initial unstable meandering jets. Left: initial potential vorticity field. Right: potential vorticity field after 100 time steps. Solid contours indicate larger values.

Newton iterations are used. The time step is 1800 s making the wave Courant number about 8.0 and the maximum advective Courant number about 3.3.

6. EFFECT OF APPROXIMATING THE JACOBIAN MATRIX

Recalculating the coefficients in (18)–(20) at each Newton iteration adds to the computational cost of this method. A number of approximations are possible that allow these coefficients to be calculated more cheaply. However, approximating these coefficients might slow the convergence of the Newton method. In this section we investigate the effect of various approximations on the convergence of the Newton iterations; this will help to determine whether such approximations might be cost effective.

DOI: 10.1002/fld

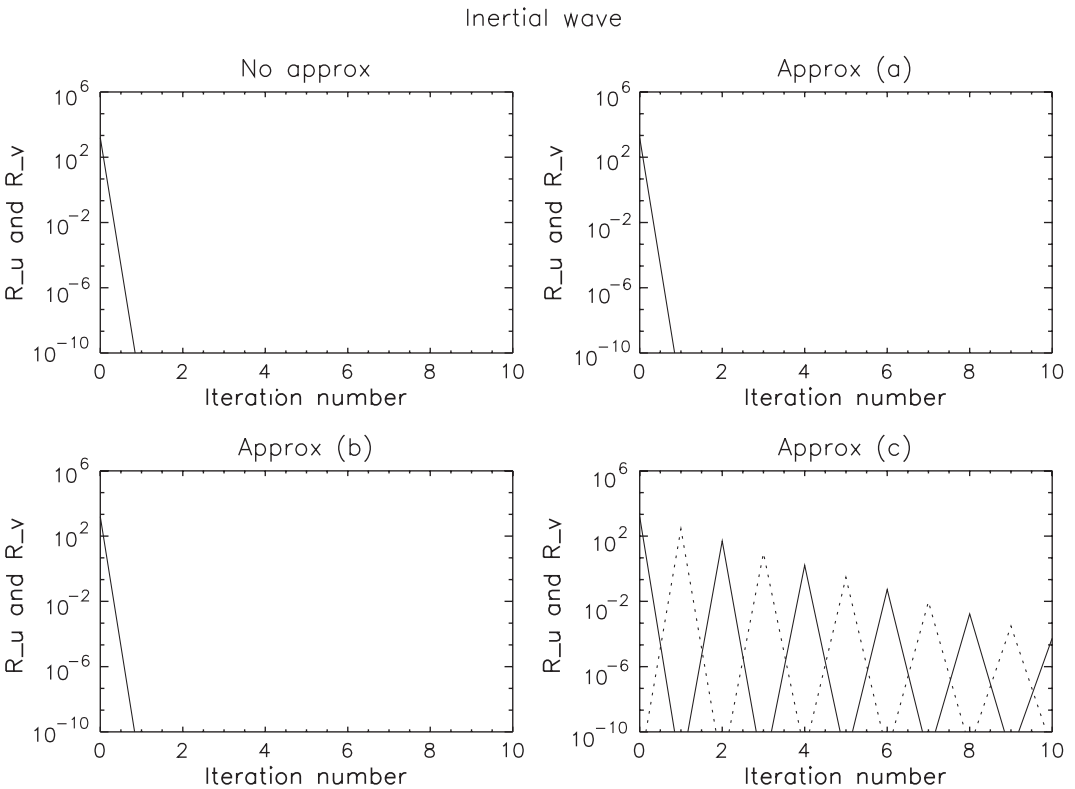

Figure 4. Newton convergence rates for inertial wave initial data. Solid and dotted curves show the root-mean-square residuals G_v and G_u, respectively. Top left: without approximation. Top right: with Group a approximations. Bottom left: with Group b approximation. Bottom right: with Group c approximation.

The possible approximations fall into three groups.

Group a: These approximations will be accurate when velocity gradients times Δt are small.

- If $|\nabla \mathbf{v}|\Delta t/2 \ll 1$, then

$$\begin{aligned} \frac{\partial x^{\mathrm{D}}}{\partial u^{\mathrm{A}}} &\approx -\frac{\Delta t}{2}, \quad \frac{\partial y^{\mathrm{D}}}{\partial u^{\mathrm{A}}} \approx 0 \\ \frac{\partial x^{\mathrm{D}}}{\partial v^{\mathrm{A}}} &\approx 0, \quad \frac{\partial y^{\mathrm{D}}}{\partial v^{\mathrm{A}}} \approx -\frac{\Delta t}{2} \end{aligned} \tag{25}$$

- If $|\xi \Delta t| \ll 1$ where $\xi = v_x - u_y$ is the relative vorticity then Lagrangian departure control volumes will not be rotated much relative to Eulerian arrival control volumes; then

$$\begin{aligned} \frac{\partial m}{\partial y} &\approx 0 \quad \text{at } u \text{ departure points} \\ \frac{\partial m}{\partial x} &\approx 0 \quad \text{at } v \text{ departure points} \end{aligned} \tag{26}$$

DOI: 10.1002/fld

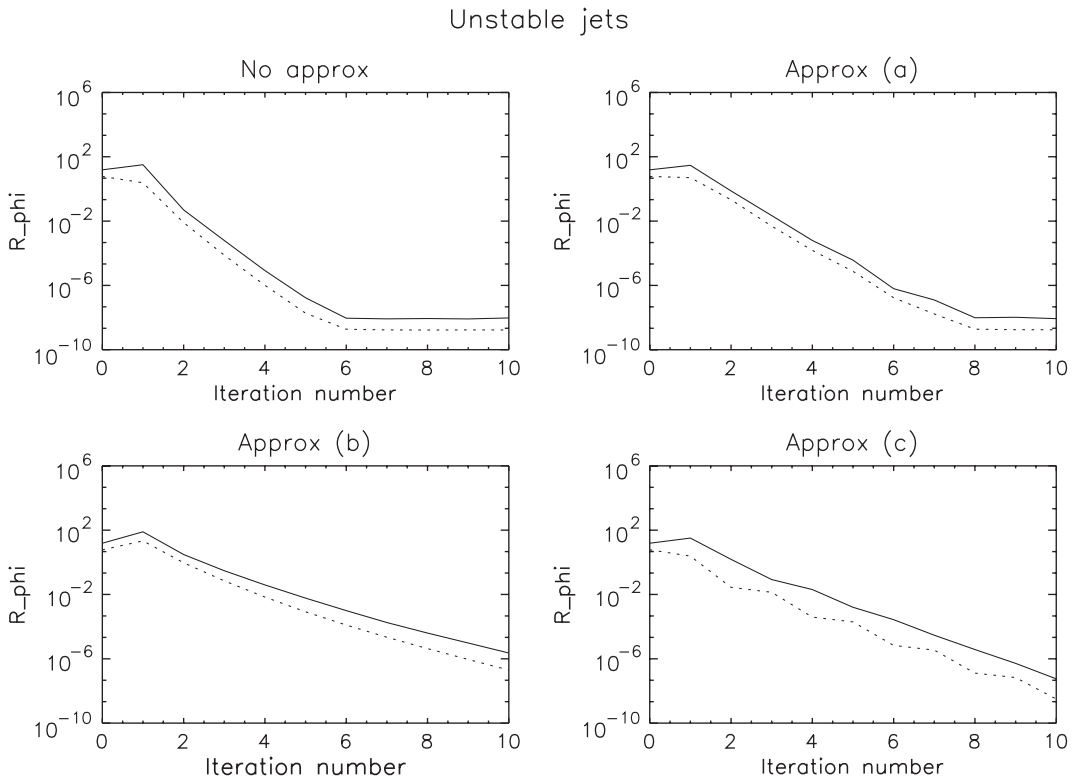

Figure 5. Newton convergence rates for meandering jet initial data. Solid and dotted curves show the maximum modulus and root-mean-square residuals G_Φ, respectively. Top left: without approximation. Top right: with Group a approximations. Bottom left: with Group b approximation. Bottom right: with Group c approximation.

- If $|\nabla \mathbf{v}|\Delta t \ll 1$, then,

$$\frac{\partial G_u}{\partial u^{\mathrm{A}}} \approx 1, \quad \frac{\partial G_v}{\partial v^{\mathrm{A}}} \approx 1 \tag{27}$$

- If $|\nabla \mathbf{v}|\Delta t \ll |f|\Delta t$ (i.e. small Rossby number) then

$$\frac{\partial G_u}{\partial \overline{v}^{\mathrm{A}}} \approx -\frac{f\Delta t}{2}, \quad \frac{\partial G_v}{\partial \overline{u}^{\mathrm{A}}} \approx \frac{f\Delta t}{2} \tag{28}$$

Group b: This approximation is valid when $|(\Phi - \Phi_0)/\Phi_0| \ll 1$ for some constant mean geopotential Φ_0, and velocity gradients times Δt are small. Then

$$\begin{aligned} \frac{\partial m}{\partial x} &\approx \Phi_0 \Delta y \quad \text{at } u \text{ departure points} \\ \frac{\partial m}{\partial y} &\approx \Phi_0 \Delta x \quad \text{at } v \text{ departure points} \end{aligned} \tag{29}$$

DOI: 10.1002/fld

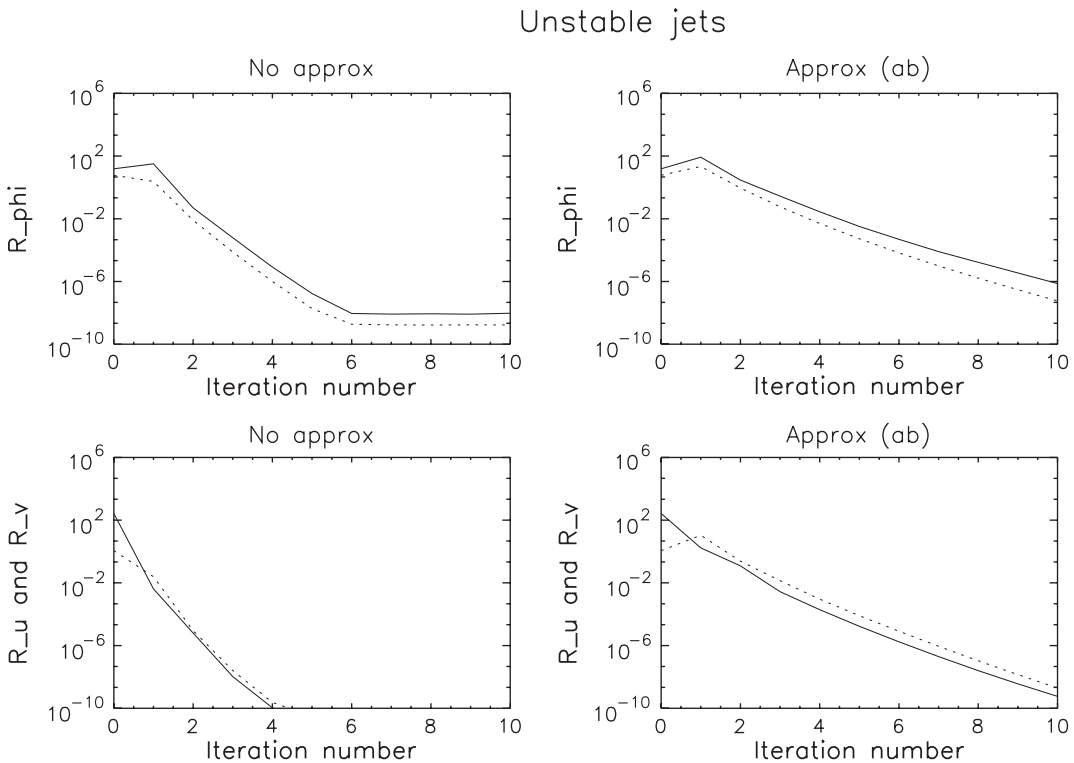

Figure 6. Newton convergence rates for meandering jet initial data. Top: solid and dotted curves show the maximum modulus and root-mean-square residuals G_Φ, respectively. Bottom: solid and dotted curves show the root-mean-square residuals G_v and G_u, respectively. Left: without approximation. Right: with Group a and Group b approximations together.

Note that this approximation re-introduces a reference geopotential in the approximate Newton method; however, the scheme (9)–(11) is insensitive to the choice of reference geopotential provided the Newton iterations converge.

Group c: This approximation is valid when $|\nabla \mathbf{v}|\Delta t \ll 1$ and $|f|\Delta t \ll 1$. Then

$$\frac{\partial G_u}{\partial \overline{v}^{\mathrm{A}}} \approx 0, \quad \frac{\partial G_v}{\partial \overline{u}^{\mathrm{A}}} \approx 0 \tag{30}$$

The effect of different combinations of approximations on the Newton convergence rate has been tested empirically for several flow regimes. A single time step is carried out, taking 10 Newton iterations, and the maximum modulus and root-mean-square of the residuals G_Φ, G_u, and G_v calculated at each iteration.

Figure 4 shows the results of one such test. The initial fields are all constant ($\Phi = 10^5\,\mathrm{m^2\,s^{-2}}$, $u = 100\,\mathrm{m\,s^{-1}}$, $v = 0\,\mathrm{m\,s^{-1}}$). The time stepping problem reduces to a linear one and the unapproximated Newton scheme converges in a single iteration. For this test, velocity gradients are zero and Φ is equal to its mean value; hence, Group a and Group b approximations should have no impact. On

DOI: 10.1002/fld

the other hand, $|f|\Delta t \approx 3.5$ is quite large so that the Group c approximation is expected to slow the Newton convergence. This is exactly what is found.

Figure 5 shows the results of a second test case. The flow field consists of balanced meandering jets, similar to those in Figure 3, but with the three dimensionless parameters $|\nabla \mathbf{v}|\Delta t$, $|\Phi - \Phi_0|/\Phi_0$, and $|f|\Delta t$ all approximately 0.2. It is unlikely that larger values of these parameters or their analogues would be met in realistic applications of a weather or climate model, so this is an extreme test. Each group of approximations is seen to result in some slowing of the Newton convergence rate. Nevertheless, in all cases the residuals are reduced by several orders of magnitude after only 3 or 4 iterations, implying that making these approximations might be cost effective.

It is particularly interesting to examine the case in which Group a and Group b approximations are made together, because the Helmholtz problem then reduces to a constant coefficient problem. Figure 6 shows results for the same test case as in Figure 5, but now comparing the convergence rate for the unapproximated case with that when Group a and Group b approximations are made together. The approximations lead to a noticeable slowing of the Newton convergence rate, but it is still fast enough that 3 or 4 iterations should be sufficient for practical use.

7. CONCLUSIONS

A fully implicit, mass-conserving, semi-Lagrangian scheme for the shallow-water equations on a doubly periodic f-plane has been proposed. The scheme avoids the introduction of a reference geopotential and treats all terms, including the trajectory calculation, in a Crank–Nicolson manner. This then leads to a nonlinear and nonlocal coupled set of equations for the predicted fields at the new time level. This coupled set can be solved by a Newton method, and because the nonlinearity is, in fact, rather weak, a small number of iterations (1–3) are sufficient for practical purposes. A key result is that the Newton iteration formula can be simplified by a partial elimination of the u and v increments to leave a near standard Helmholtz problem for the Φ increments, for which efficient solution methods are well known.

The method has been implemented and tested and is found to work well even for large wave and advective Courant numbers. In theory the method should work and remain stable provided $|\nabla \mathbf{v}|\Delta t/2$ is less than about 1 to ensure that back trajectories do not become tangled.

The impact on the Newton convergence rate of approximating terms in the Jacobian matrix has been investigated. The Newton convergence rate is noticeably slowed by the approximations examined, but is still fast enough to be practically useful. Approximations that lead to a constant coefficient Helmholtz problem are particularly attractive because they may permit very efficient solution methods.

A three-dimensional spherical version of SLICE has been developed at the Met Office. It appears possible, therefore, to extend the methodology described here to the compressible Euler equations in three-dimensional spherical geometry for use in operational weather and climate models.

ACKNOWLEDGEMENTS

This work was supported in part by the Met Office. Discussions with the Met Office Dynamics Research group were particularly useful during the course of this work, and comments of two anonymous reviewers were valuable for improving the presentation.

DOI: 10.1002/fld

REFERENCES

1. Lauritzen PH, Kaas E, Machenhauer B. A mass-conservative semi-implicit semi-Lagrangian limited-area shallow-water model on the sphere. *Monthly Weather Review* 2006; **134**:1205–1221.
2. Williamson DL, Drake JB, Hack JJ, Jakob R, Swarztrauber PN. A standard test set for numerical approximations to the shallow-water equations in spherical geometry. *Journal of Computational Physics* 1992; **102**:211–224.
3. Arakawa A, Lamb VR. Computational design of the basic dynamical processes of the UCLA general circulation model. In *General Circulation Models of the Atmosphere*, Chang J (ed.). Methods in Computational Physics, vol. 17. Academic Press: San Diego, 1977; 173–265.
4. Robert A. The integration of a spectral model of the atmosphere by the implicit method. *Proceedings of the WMO/IUGG Symposium on NWP in Tokyo*, Japan Meteorology Agency, Tokyo, Japan, 1969; VII.19–VII.24.
5. Staniforth AN, Côté J. Semi-Lagrangian schemes for atmospheric models—a review. *Monthly Weather Review* 1991; **119**:2206–2223.
6. Cullen MJP, Salmond DJ. On the use of a predictor-corrector scheme to couple the dynamics with the physical parameterizations in the ECMWF model. *Quarterly Journal of the Royal Meteorological Society* 2003; **129**: 1217–1236.
7. Leonard BP, Lock AP, MacVean MK. Conservative explicit unrestricted-time-step multidimensional constancy-preserving advection schemes. *Monthly Weather Review* 1996; **124**:2588–2606.
8. Lin S-J, Rood RB. Multidimensional flux-form semi-Lagrangian transport schemes. *Monthly Weather Review* 1996; **124**:2046–2070.
9. Nair RD, Machenhauer B. The mass-conservative cell-integrated semi-Lagrangian advection scheme on the sphere. *Monthly Weather Review* 2002; **130**:649–667.
10. Zerroukat M, Wood N, Staniforth A. SLICE: a semi-Lagrangian inherently conserving and efficient scheme for transport problems. *Quarterly Journal of the Royal Meteorological Society* 2002; **128**:2801–2820.
11. Zerroukat M, Wood N, Staniforth A. Application of the parabolic spline method (PSM) to a multidimensional conservative semi-Lagrangian transport scheme (SLICE). *Journal of Computational Physics* 2007; **225**:935–948.
12. Fulton SR, Ciesielski PE, Schubert WH. Multigrid methods for elliptic problems—a review. *Monthly Weather Review* 1986; **114**:943–959.

DOI: 10.1002/fld